

Article

Luminescence Properties of LaAlO₃:Pr under Hydrostatic Pressure

Nurgul Zhanturina ^{1,*}, Gulnara Beketova ¹, Natalia Gorecka ², Karol Szczodrowski ², Tadeusz Lesniewski ², Zukhra Aimaganbetova ¹, Karlygash Bizhanova ³ and Amirbek Bekeshev ¹

¹ Department of Physics, K.Zhubanov Aktobe Regional University, Aktobe 030000, Kazakhstan; diko_2006@mail.ru (G.B.); zukhra.aimaganbetova@mail.ru (Z.A.)

² Institute of Experimental Physics, University of Gdansk, 80-308 Gdansk, Poland;

natalia.gorecka@ug.edu.pl (N.G.); karol.szczodrowski@ug.edu.pl (K.S.); tadeusz.lesniewski@ug.edu.pl (T.L.)

³ Department of Fundamental Sciences, Yessenov University, Aktau 130000, Kazakhstan; bizhanovakar@mail.ru

* Correspondence: nzhanturina@mail.ru; Tel.: +77-013684899

Abstract: The article presents the results of measuring the luminescence spectra, luminescence excitation spectra and luminescence spectra under high pressures for LaAlO₃:Pr with concentration of 1%. The materials were synthesized by solid phase synthesis. Diffraction pattern is fully relates to LaAlO₃ phase. The photoluminescence spectra show the main energy transitions. The change in the position of the main bands under the hydrostatic pressure of 23, 55, 160 and 191 kBar was demonstrated. The main band at 491 nm is slightly red-shifted, while the line at 605 nm is shifted to the high-energy part of the spectrum. The intensity of all bands increases with increasing hydrostatic pressure. The dynamics of changes in the intensities of maxima and emissions from different transitions are analyzed. Studies of luminescence under high hydrostatic compression are important in observing changes in the internal structure and electronic states of materials under the influence of high pressure, studying internal processes such as recombination of electrons and holes, transitions between energy levels and the release of photons. Understanding the changes that occur under compression can help researchers develop new materials with unique properties.

Keywords: perovskites; photoluminescence; photoluminescence excitation spectra; hydrostatic pressure



Citation: Zhanturina, N.; Beketova, G.; Gorecka, N.; Szczodrowski, K.; Lesniewski, T.; Aimaganbetova, Z.; Bizhanova, K.; Bekeshev, A.

Luminescence Properties of LaAlO₃:Pr under Hydrostatic Pressure. *Crystals* **2023**, *13*, 1558. <https://doi.org/10.3390/cryst13111558>

Academic Editor: László Kovács

Received: 23 September 2023

Revised: 24 October 2023

Accepted: 29 October 2023

Published: 1 November 2023



Copyright: © 2023 by the authors. Licensee MDPI, Basel, Switzerland. This article is an open access article distributed under the terms and conditions of the Creative Commons Attribution (CC BY) license (<https://creativecommons.org/licenses/by/4.0/>).

1. Introduction

Recently, the optical properties of perovskites have been intensively studied due to the fact that, depending on the shape of the crystals, perovskites can exhibit anisotropy. Scientists have discovered that, under certain conditions, perovskites have a record high level of optical anisotropy for all known three-dimensional materials. This makes it possible to use perovskites to create highly efficient waveguides and other devices that control the movement of light, which is extremely important for creating optical analogues of electronics [1]. Various properties of minerals, such as ferroelectricity, photoluminescence, superconductivity, nonlinear optical properties and magnetoresistance of perovskites [2] attract special attention, and interest in nanocrystalline systems of complex chemical composition is also growing. Particular attention is paid to complex oxide compounds due to their practical importance. Thus, perovskites, garnets, molybdates and borates of rare earth elements (REE) have effective scintillator properties [3].

There are also studies where luminescent perovskites have important applications in the fields of nonlinear optical properties, solar cells, scintillators, lighting devices, photocatalysts [4], water splitting, generation and electronic devices (e.g., capacitors, converters, drives).

The center of trivalent praseodim (Pr³⁺) attracts attention as a luminescent center of scintillators. It is somewhat more resistant to corrosion in air than europium, lanthanum or

cerium, but readily forms a green oxide layer that flakes off in air. At 798 °C, hexagonal α -Pr transforms into body-centered cubic β -Pr.

Since Pr^{3+} , like some rare earth elements, has a relatively short decay time and high radiation efficiency, the greatest interest is in the development of Pr^{3+} doped scintillators with high sensitivity [5] to various types of ionizing radiation. It is assumed that the synthesized $\text{LaAlO}_3:\text{Pr}^{3+}$ can be used for dosimetry of ionizing radiation using the thermoluminescence method.

Scientists have studied the photoluminescence spectra and luminescence excitation spectra (PLE) of praseodymium [6]. Stokes photoluminescence spectra [7] at different energies of exciting photons, as well as X-ray and cathodoluminescence spectra contain a set of broad bands and lines corresponding to 97 radiative transitions in Pr^{3+} ions, as well as a luminescence band associated with a defect. All radiative transitions and electronic states of Pr^{3+} ions were determined using the Dicke energy diagram for the Pr^{3+} ion [8].

Thus, doping the material increases the emission centers and the transfer of energy from the matrix to the luminescence centers [9]. Therefore, from an academic point of view, the study of new Pr-doped materials is of great interest. Perovskites doped with Pr^{3+} ions are of great interest as a phosphor for converting LED light into white light sources [10].

In current paper we consider the properties of luminescence under the hydrostatic pressure. Research on luminescence under high hydrostatic compression is of great importance in various scientific and technical fields. Hydrostatic compression can create extreme conditions that greatly change the properties of materials. Luminescence studies allow one to observe changes in the internal structure and electronic states of materials under the influence of high pressure [11]. In some cases, increasing hydrostatic pressure enhances the intensity of luminescence. This phenomenon is known as positive pressure sensitivity. It is often observed in materials that have a crystalline structure with well-defined energy levels and can withstand pressure without damage. Under increased pressure, the energy levels in these materials can shift, leading to an increase in the energy gap between electronic states. This increased energy gap can result in more intense and higher-energy luminescence [12–14].

Also, under the influence of high hydrostatic compression, materials can change from one phase to another. The study of luminescence makes it possible to determine the moments of phase transitions and associated changes in structure and properties. Understanding the changes that occur under compression can help researchers develop new materials with unique properties. For example, the creation of new photoactive or optical materials that can be used in various applications, including electronics, optics and photonics. Luminescence allows one to study internal processes such as the recombination of electrons and holes, transitions between energy levels, and the release of photons. This can lead to a better understanding of the fundamentals of electronics and optics. High-pressure luminescence studies can have practical applications in various fields, such as geology (the study of the properties of minerals under pressure), materials science (the development of new materials) and high-pressure physics (the study of phase diagrams). Overall, studies of luminescence under high hydrostatic compression expand our knowledge of the behavior of materials under extreme conditions and may have important practical applications in various fields of science and technology [15].

The purpose of the study is to study the photoluminescence spectra, photoluminescence excitation spectra in $\text{LaAlO}_3:\text{Pr}$ (1%) under the influence of hydrostatic compression to determine the processes of energy transfer from luminescence centers to the original matrix and analyze the luminescence intensities and bands.

2. Materials and Methods

$\text{LaAlO}_3:\text{Pr}$ sample were synthesized using Pechini method at the Institute of Experimental Physics of the University of Gdansk (Poland). Details of the synthesis procedure are described in the work of A. Watras et al. [16]. The praseodymium ions (1% of moles) were intentionally incorporated into the lanthanum sites in the matrix. To obtain the desired aluminate, the following reagents were used: $\text{La}(\text{NO}_3)_2 \times 6\text{H}_2\text{O}$ (99.99%), $\text{Al}(\text{NO}_3)_3 \times 9\text{H}_2\text{O}$ (99.997%), $\text{Pr}(\text{NO}_3)_3 \times 6\text{H}_2\text{O}$ (99.9%), citric acid and ethylene glycol. The reagents were

purchased from Sigma-Aldrich. In the first step, the citric acid was dissolved in distilled water and then the appropriate amount of ethylene glycol was added to the acid solution to keep the acid/glycol molar ratio equal to 5:1. Next the lanthanum, aluminum and praseodymium nitrates, previously dissolved in distilled water, were added to the obtained acid–glycol solution. In the second step of synthesis the prepared mixture was heated for 1 h at 100 °C under reflux to perform an esterification process. Then, the prepared polyester was dried at 80 °C for 24 h and then the prepared dry polyester was calcined at 1100 °C for 4 h under neutral atmosphere in a tubular furnace (Nabertherm, RHTH 120-600/18).

By X axis of XRD spectra is the 2 Theta (2Q), when Q—is the angle of reflection of X-rays. The Y axis of an XRD pattern correspond to the intensity of signal and it is presented in counts per acquisition step. In figure we specified the PDF Card number by which we have identified the phases. Red lines correspond to the phase of LaAlO₃. So as we see the sample with 1% of praseodymium contains 100% LaAlO₃ phase.

The phase purity of the material were characterized by X-ray diffraction using BRUKER D2PHASER equipment. D2 PHASER has a simple circuit consisting of an ultracompact goniometer, an X-ray tube, a high-voltage generator, X-ray beam generation systems and a high-speed semiconductor detector LYNXEYE. The standard X-ray tube uses 1/6 of its nominal power, is equipped with a water-cooling cycle. The XRD patterns were collected using a scanning step of 0.02° and a counting time of 0.4 s per step. The analysis of the obtained results was carried out using a DIFFRAC.EVA V4.1 evaluating application from the BRUKER. The XRD pattern recorded for the obtained product is presented in Figure 1. It shows that the collected pattern matches very well to the desired phase of LaAlO₃ attributed to the 04-006-0695 powder diffraction file. The main peak of the cubic LaAlO₃:Pr structure is centered at 2Θ = 33.5°. The lattice constant is 3.78 Å. Some other XRD diffraction lines, located at 23.5°, 41.5°, 48°, 54.2°, 55.11°, 59.7° and others. The signal at 50.05° is the instrumental artefact. Taking into account the obtained result it can be concluded that the sample doped with 1% of mole of praseodymium contains 100% of LaAlO₃ phase.

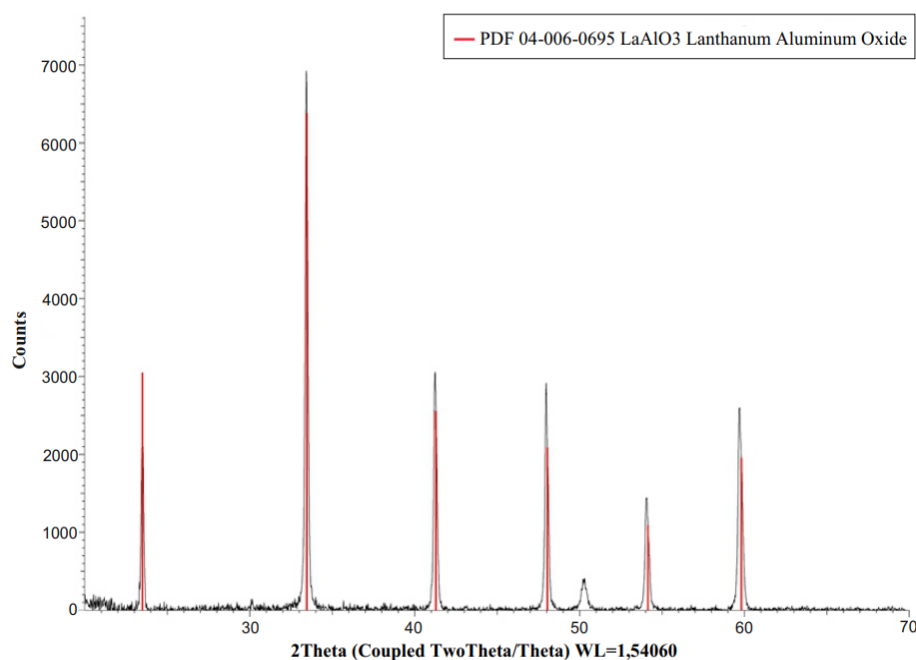


Figure 1. X-ray diffraction spectra of LaAlO₃:Pr.

The particle sizes are calculated using the Scherrer equation:

$$d = \frac{K\lambda}{\beta \cos\theta}$$

where d —average size of particles, K —Scherers constant (0.89), λ —X ray wavelength, β —line broadening at half the maximum intensity (FWHM), (in radians, 2θ); θ —is the Bragg angle [17,18].

The results of calculations of particle size are presented in Table 1.

Table 1. The quantitative analysis of LaAlO₃ samples doped with praseodymium.

%	λ	2θ	β	d (nm)
1	1.5406 Å	33.463	0.05	29

So, the average particle size of Pr doped LaAlO₃ is 29 nm.

Room temperature (RT) photoluminescence excitation (PLE) spectra of powder samples were measured with a FluoroMax-4P spectrofluorometer (Horiba, Kyoto, Japan) equipped with a 150 W xenon lamp as an excitation source and a R928 Hamamatsu photomultiplier as a detector which allows recording PL and PLE spectra in the spectral range of 250–850 nm. At the PL measuring the excitation wavelength was 390 nm.

Photoluminescence emission spectra were measured using the excitation source of He—Cd laser at 442 nm. Each sample was measured at the room temperature (295 K). The room temperature excitation spectra were measured with a FluoroMax-4P (Horiba) spectrofluorimeter equipped with a Hamamatsu R928 photomultiplier, 150 W ozone-free xenon lamp, which allows to record spectrum in the range of 250–850 nm. Low temperature spectra were measured using 0.75 m focal length Czerny-Turner grating spectrometer Shamrock SR750 D1 with an iDus 420 CCD detector (Andor Technology, Belfast, UK). For cryogenic temperature the samples were held in DE-202 closed cycle helium cryostat (ARS Cryo, Macungie, PA, USA).

The experimental setup for creating high hydrostatic pressure consists of helium-cadmium (He-Cd) lasers with a wavelength of 325 nm, a 150 mW xenon lamp for excitation of luminescence, a PGS2 spectrometer operating as a monochromator, a Hamamatsu model R943-2 photomultiplier operating in counting mode photons. Pressure is generated using a miniature Merrill Basset-type diamond anvil (AD), which can generate high hydrostatic pressures of up to 400 kbar. and can be loaded into a helium cryostat (Figure 1). The device for loading AD consists of optical microscopes OYMPUSSZ×10 and a micrometer substrate Miltutoyo.

3. Results

Luminescence properties of LaAlO₃:Pr have been investigated in the 250–800 nm region at room temperature. Figure 2 shows the luminescence excitation spectrum of LaAlO₃:Pr under ambient conditions. The monitored excitation wavelengths were carefully chosen to achieve the best possible separation of the spectra related with different cation sites and were set at 631 nm.

The excitation channels in the UV are hardly observable, while the optical transitions from the ground state to the ³P_J manifolds are clearly visible, with maxima localized at 448.5, 470 and 489 nm. They correspond to optical transitions from the ground state to 3P_J. (³H₄ → ³P_J + ¹I₆)

Next figure demonstrates the photoluminescence spectra (PL) of crystal for excitation at 449 nm (Figure 3).

As an excitation wavelength we choosed 449 nm because it is in short-wavelength spectral range, that is characteristic for material under consideration. The emission spectrum, presented in Figure 3, has completely different characters, exhibiting the presence of several narrow-band emission lines. In the case of praseodymium-doped sample, the main emission band is near the excitation (if we compare 492 nm and 471 nm), therefore less efficient excitation via ³P₂ level at 449 nm was used in the following measurements. The sharp and narrow bands peaked at lower energies (over 450 nm) are directly associated with the presence of the lanthanide ion Pr³⁺. The band at 491 dominates in PL spectra,

which corresponds to the transition ${}^3P_0 \rightarrow {}^3H_4$, which is complemented by minor maxima in the green region at 529 nm and 545 nm, orange 605 nm and 612 nm, also 654 nm. The most intense peak at 491 nm corresponds to the $4f_2 - 4f_5d$ transitions with the slight contribution of the La^{3+} [19]. The majority of bands corresponds to the transitions from 3P_0 , 492 nm— ${}^3P_0 \rightarrow {}^3H_4$, 529 nm and 545 nm— ${}^3P_0 \rightarrow {}^3H_5$, 613 nm— ${}^3P_0 \rightarrow {}^3H_5$, 654 nm— ${}^3P_0 \rightarrow {}^3F_2$. However there is also observable a trace of emission from 1D_2 level—605 nm [20]. The ${}^3P_0 \rightarrow {}^3H_4$, ${}^3P_0 \rightarrow {}^3H_4$ transitions showed higher intensity than the corresponding, whereas ${}^3P_0 \rightarrow {}^3F_2$, from 1D_2 level exhibited the lower intensities.

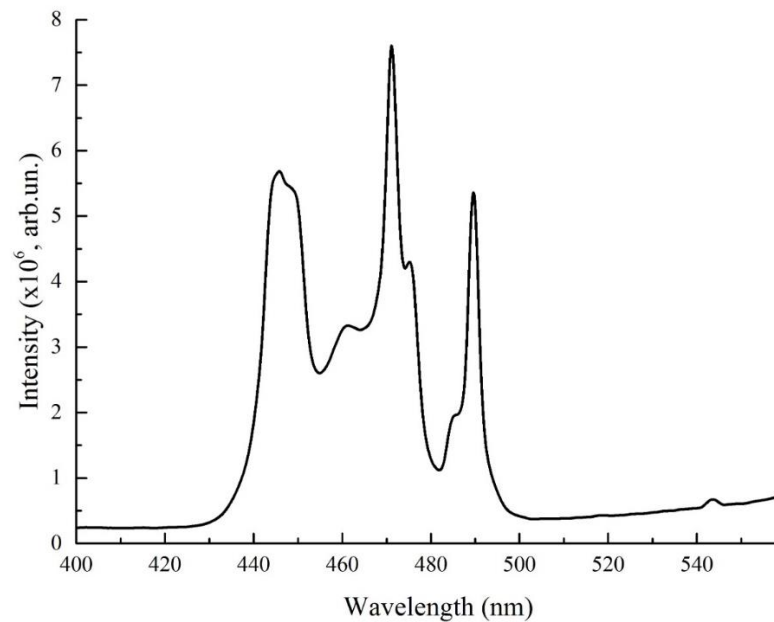


Figure 2. Photoluminescence excitation spectra of $\text{LaAlO}_3:\text{Pr}$.

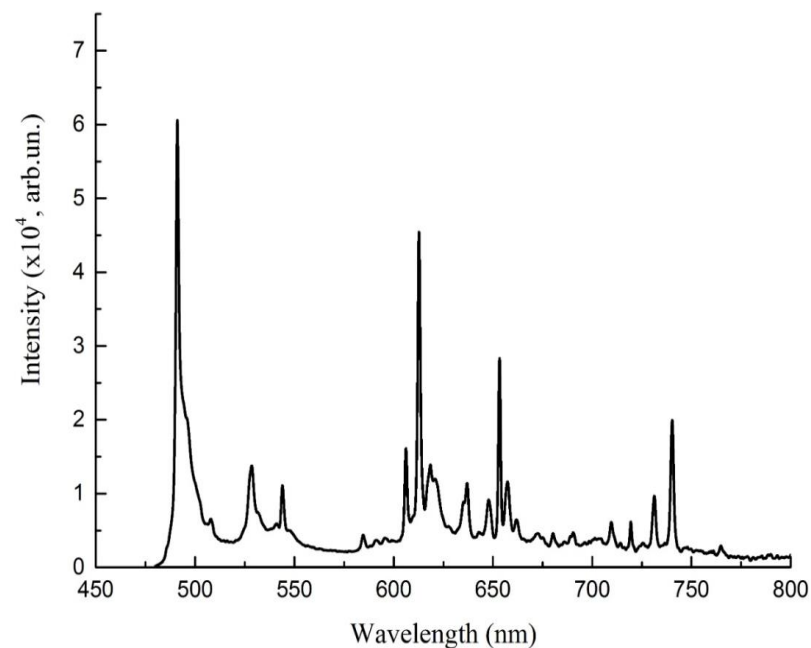


Figure 3. Photoluminescence spectra of $\text{LaAlO}_3:\text{Pr}$ for excitation at 449 nm.

We investigate the PL spectra of crystals under the hydrostatic pressure (Figure 4). The application of hydrostatic pressure is a unique tool to test some conditions, locations of the bands, their redshift or blueshift, change in intensity, energy distributions between different states.

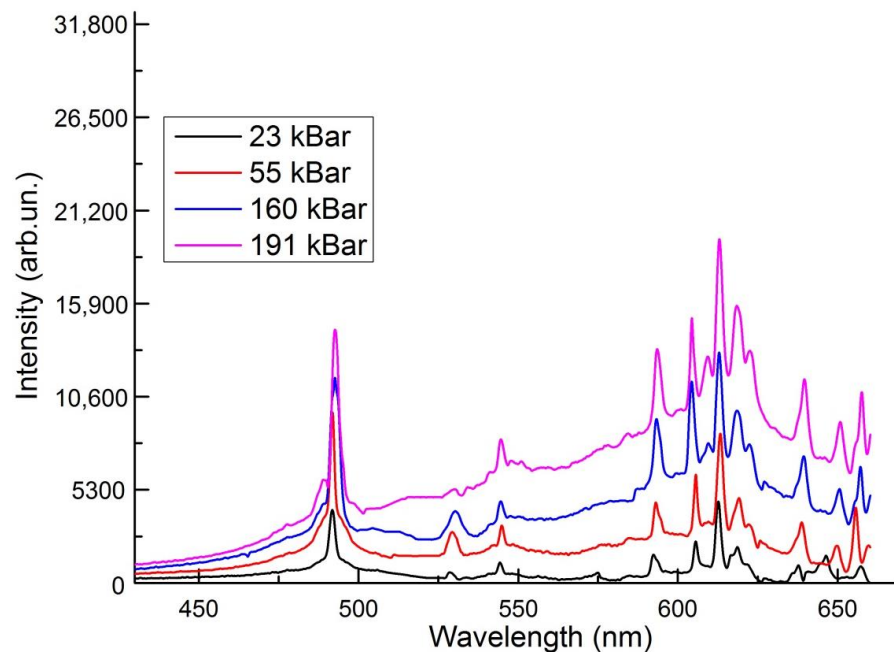


Figure 4. PL spectra of LaAlO₃:Pr under the hydrostatic pressure.

The main emission peak at 491 nm do not change dramatically in bandwidth, but the position changes slightly. From 23 to 191 kBar it changes from 491.8 nm to 492,66 nm, which corresponds to pressure shift of -0.026 meV/kbar, i.e., energy reduces. The luminescence band at ambient pressure appears at 528.5 nm, at 23 kBar—528.5 nm, 55 kBar —529.4 nm, 160 kBar—530.3 nm, 191 Kbar—530.3 nm. The redshift is considered for this line. The position of bands at 545 nm, 612 nm and 654 nm experiences slightly shift to the right, but not permanently. For example, lines at 545 nm and 612 nm from 23 kBar to 55 kBar are shifted to red region, from 55 kBar to 160 kBar—blue region and stays constantly at 190 kBar. The situation is different for the emission band at 605 nm, with pressure increasing it moves to the high energy site of the spectra.

Low pressure coefficients were found indicating the involvement of highly localized states in the process of radiative recombination. It can be seen that with increasing pressure at 160 kBar, a band appears at 609 nm, the intensity of which becomes greater at 191 kBar. The appearance of this band is explained by the redistribution of energy from transitions from 3P_0 states to transitions from 1D_2 states.

Under normal conditions, the luminescence spectra consist of bands corresponding to transitions from excited 1D_2 level, whereas luminescence from the higher excited level 5D_3 Pr³⁺ ion is not observed. When the pressure reaches 160 kbar, additional luminescence lines appear corresponding to the redistribution of energy from the 1D_3 state.

We can connect this fact with pressure induced low-symmetry crystal-field effects.

The decrease in the energy difference between excited and ground state configurations is normally caused by increasing interactions of the emitting ion with its local environment due to decreasing interatomic distances under pressure [21]. Pressure (by reducing the interionic distances) can change the relative contributions to the effective field, that in specific cases can reduce the splitting of electronic configuration. As a result in specific environments a blue or red shift of the emission band can be observed [22]. The change in symmetry can influence the interband transition efficiency of praseodymium ion [23].

The energy of the zero-phonon line decreases with the increase in hydrostatic pressure, which is typical for lanthanide ions. The pressure due to the reduce in interatomic distances leads to an increase of the interaction of 4fn electrons with ligand electrons and diminishes the quantities of Racah parameters and spin–orbit coupling. The crystal compression causes an increase in crystal stiffness and phonon energies. Therefore the pressure shifts of phonon repetition lines are smaller than the respective shift of zero-phonon line [24].

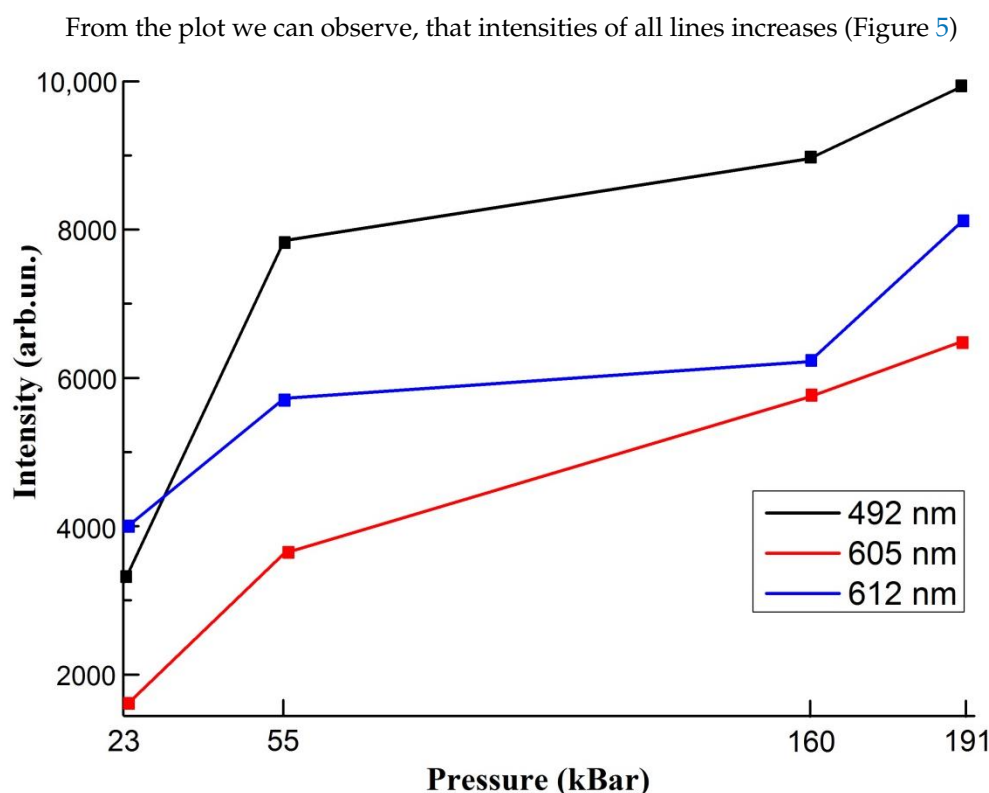


Figure 5. Intensities of bands at different hydrostatic pressure values.

From the figure above we can observe, that pressure leads to the increase in intensity of all lines. From 23 to 55 kBar the change in intensity is more than 1.5 times, from 55 kBar to 160 kBar there are no sufficient increase. Further enhancement in luminescence is insignificant in the case of 612 nm band. The intensity is nearly constant after $p > 55$ GPa, but before from 23 kBar to 55 kBar it was experienced the significant growth. This effect is related to the approaching of transition pressure. The width at half maximum, on the other hand, increases continuously with P . According to the configuration coordinate model, the pressure-induced variation of the width at half maximum is related to parameters characterizing the electron-lattice coupling. The model predicts a linear increase of the width with pressure.

For all pressure the dominating spectral lines correspond to the transition from the 3P_0 state to the 3H_4 , 3H_5 and 2F_3 states. Initially, the emission from the 1D_2 state is weaker. It can be noticed that the relative intensity of the $^1D_2 \rightarrow ^3H_4$ emission increases with increasing pressure and is related to increase of non-radiative $^3P_0 \rightarrow ^1D_2$ transition that leads to the redistribution of energies between 3P_0 and 1D_2 state.

This effect is seen in Figure 6, where relative intensity of the emission from the 3P_0 (491 nm) to the intensity of emission from 1D_2 state (605 nm) versus pressure is presented [25].

It is clearly observable the relative quenching of the emission from 491 nm and enhancing of the emission from 605 nm band.

It can be noticed that with increasing pressure, the band at 605 nm, which corresponds to the transition from the 1D_2 state, shifts to shorter wavelengths site (Table 2).

Table 2. The shift of the emission 605 nm with pressure.

P, kBar	23	55	160	191
Wavelength, nm	605.62	605.62	604.33	603.03

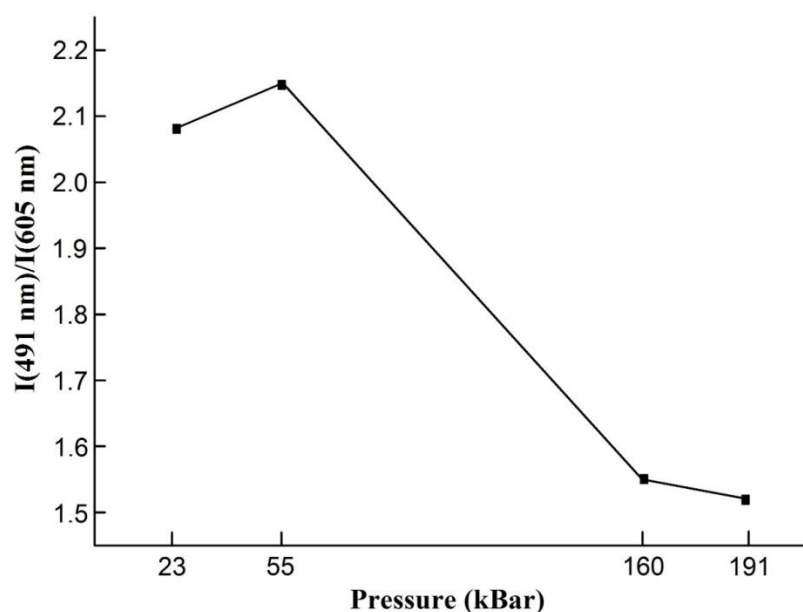


Figure 6. The dependence of relation of the intensity from 3P_0 state to 1D_2 state.

If we calculated bandshift with pressure in wavenumbers it exceeds about $0.33 \text{ cm}^{-1}/\text{kBar}$ from 55 to 160 kBar and $1.16 \text{ cm}^{-1}/\text{kBar}$ from 160 kBar to 191 kBar. For comparison in paper [13] shift is around $0.8 \text{ cm}^{-1}/\text{kBar}$, in [26]— $0.26 \text{ cm}^{-1}/\text{kBar}$, in [27]— $0.4 \text{ cm}^{-1}/\text{kBar}$. Pressure shifts of the emission lines related to the lanthanides transitions are usually not greater than a single $\text{cm}^{-1}/\text{kbar}$. This uncommon behavior can be linked to pressure induced phase transition occurring in LaAlO_3 around 136 kbar [26].

4. Conclusions

Materials used in the research were prepared by solid state synthesis method, for the recovery atmosphere the graphite tiles are used. As you see by the diffraction analysis pattern the sample contains 100% of LaAlO_3 phase.

From the photoluminescence excitation spectra we see optical transitions from the ground state to 3P_j —maxima at 448.5, 470 and 489 nm.

In emission spectra for $\text{LaAlO}_3: \text{Pr}^{3+}$ the transitions from 3P_j manifolds entirely dominate the spectra. In spectra of photoluminescence of $\text{LaAlO}_3:\text{Pr}$ samples there are 6 main bands— at 491 nm, 529 nm, 545 nm, 605 nm, 612 nm and 654 nm are registered. They correspond to the transitions from 3P_0 state. Only band at 607 nm—from 1D_2 level.

The main peak at 491 nm experiences redshift under hydrostatic. From 23 to 191 kBar it changes from 491.8 nm to 492.66 nm, which corresponds to pressure shift of $-0.026 \text{ meV}/\text{kbar}$. The appearance of emission band at 609 nm is explained with pressure induced low-symmetry crystal-field effects. Hydrostatic pressure influence leads to the enhancing in luminescence intensity.

However, the line at 605 nm tends to change position to high energy site which can be linked to pressure induced phase transition occurring in LaAlO_3 .

The emission from 3P_0 state quenches and emission from 1D_2 state magnifies with increase in pressure. The calculated relation of the intensity of 491 nm band to 605 band demonstrates the weakening of emission from 3P_0 with hydrostatic pressure increase. The nonradiative relaxation becomes more effective.

Studies of luminescence under high hydrostatic compression are important in observing changes in the internal structure and electronic states of materials under the influence of high pressure, studying internal processes such as recombination of electrons and holes, transitions between energy levels and the release of photons.

The results from the study of $\text{LaAlO}_3:\text{Pr}$ subjected to hydrostatic compression may have several important applications and benefits. Changing optical transparency, energy levels, and spectral characteristics is important when creating materials for optical and

photonic applications. LaAlO₃:Pr can be used as a pressure-sensing sensor material, that is, to develop sensors that measure pressure in various applications. LaAlO₃:Pr is a potentially efficient material in solar cells and other energy devices. The results of studying changes in luminescence under hydrostatic pressure can lead to improved efficiency of energy conversion processes.

Author Contributions: Conceptualization, N.Z. and T.L.; methodology, Z.A.; software, A.B.; validation K.B.; formal analysis, Z.A.; investigation, N.Z. and N.G.; resources, K.S. and G.B. data curation; writing—original draft preparation, N.Z. and G.B.; writing—review and editing, N.Z.; visualization, Z.A.; supervision, N.Z.; project administration, K.B. All authors have read and agreed to the published version of the manuscript.

Funding: This research was funded by the Ministry of Science and Higher Education of the Republic of Kazakhstan by project No. AP09057946 “Spectroscopic studies of functional materials based on perovskites and garnets doped with Ln²⁺, Ln³⁺, Ln⁴⁺”.

Informed Consent Statement: Informed consent was obtained from all subjects involved in the study.

Data Availability Statement: The data presented in this study are available through email upon request to the corresponding author.

Conflicts of Interest: The authors declare no conflict of interest.

References

1. Rizwan, M.; Gul, S.; Iqbal, T.; Mushtaq, U.; Farooq, M.H.; Farman, M.; Bibi, R.; Ijaz, M. A review on perovskite lanthanum aluminate (LaAlO₃), its properties and applications. *Mater. Res. Express* **2019**, *6*, 112001. [[CrossRef](#)]
2. Jain, U.; Soni, S.; Chauhan, N. Application of perovskites in bioimaging: The state-of-the-art and future developments. *Expert Rev. Mol. Diagn.* **2022**, *22*, 867–880. [[CrossRef](#)] [[PubMed](#)]
3. Song, X.; Chang, M. Rare-Earth Elements in Lighting and Optical Applications and Their Recycling. *JOM* **2013**, *65*, 1276–1282. [[CrossRef](#)]
4. Bresolin, B.M.; Park, Y.; Bahnemann, D.W. Recent Progresses on Metal Halide Perovskite-Based Material as Potential Photocatalyst. *Catalysts* **2020**, *10*, 709. [[CrossRef](#)]
5. Jana, A.; Cho, S.; Patil, S.A.; Meena, A.; Jo, Y.; Sree, V.G.; Park, Y.; Kim, H.; Im, H.; Taylor, A. Perovskite: Scintillators, direct detectors, and X-ray imagers. *Mater. Today* **2022**, *55*, 100–136. [[CrossRef](#)]
6. Song, Z.; Zhao, J.; Liu, Q. Luminescent perovskites: Recent advances in theory and experiments. *Inorg. Chem. Front.* **2019**, *6*, 2969–3011. [[CrossRef](#)]
7. Gan, Z.; Chen, W.; Lin, Y.; Cao, G.; Zhou, C.; Huang, S.; Wen, H.; Jia, B. External Stokes shift of perovskite nanocrystals enlarged by photon recycling. *Appl. Phys. Lett.* **2019**, *114*, 011906. [[CrossRef](#)]
8. Chen, D.; Chen, X. Luminescent perovskite quantum dots: Synthesis, microstructures, optical properties and applications. *J. Mater. Chem. C* **2019**, *7*, 1413–1446. [[CrossRef](#)]
9. Zhang, W.; Yang, S.; Li, J.; Gao, W.; Deng, Y.; Dong, W.; Zhao, C.; Lu, G. Visible-to-ultraviolet Upconversion: Energy transfer, material matrix, and synthesis strategies. *Appl. Catal. B Environ.* **2017**, *206*, 89–103. [[CrossRef](#)]
10. Ye, S.; Xiao, F.; Pan, Y.X.; Ma, Y.Y.; Zhang, Q.Y. Phosphors in phosphor-converted white light-emitting diodes: Recent advances in materials, techniques and properties. *Mater. Sci. Eng. R.* **2010**, *71*, 1–34. [[CrossRef](#)]
11. Hernández-Rodríguez, M.A.; Muñoz-Santiuste, J.E.; Lavín, V.; Lozano-Gorrín, A.D.; Rodríguez-Hernández, P.; Muñoz, A.; Venkatramu, V.; Martín, I.R.; Rodríguez-Mendoza, U.L. High pressure luminescence of Nd³⁺ in YAlO₃ perovskite nanocrystals: A crystal-field analysis. *J. Chem. Phys.* **2018**, *148*, 044201. [[CrossRef](#)] [[PubMed](#)]
12. Wang, L.; Ye, K.-Q.; Zhang, H.-Y. Organic materials with hydrostatic pressure induced mechanochromic properties. *Chin. Chem. Lett.* **2016**, *27*, 1367–1375. [[CrossRef](#)]
13. Mahlik, S.; Lazarowska, A.; Grinberg, M.; Liu, T.-C.; Liu, R.-S. Luminescence Spectra of β-SiAlON/Pr³⁺ Under High Hydrostatic Pressure. *J. Phys. Chem. C* **2013**, *117*, 13181–13186. [[CrossRef](#)]
14. Lazarowska, A.; Mahlik, S.; Grinberg, M.; Li, G.; Liu, R.-S. Structural phase transitions and photoluminescence properties of oxonitridosilicate phosphors under high hydrostatic pressure. *Sci. Rep.* **2016**, *6*, 34010. [[CrossRef](#)]
15. Chen, K.C.; Fang, M.H.; Huang, W.T.; Kamiński, M.; Majewska, N.; Leśniewski, T.; Mahlik, M.; Leniec, G.; Kaczmarek, S.M.; Yang, C.W.; et al. Chemical and Mechanical Pressure-Induced Photoluminescence Tuning via Structural Evolution and Hydrostatic Pressure. *Chem. Mater.* **2021**, *33*, 3832–3840. [[CrossRef](#)]
16. Watras, A.; Deren, P.J.; Pazik, R.; Maleszka-Baginska, K. Upconversion luminescence properties of nanocrystallite MgAl₂O₄ spinel doped with Ho³⁺ and Yb³⁺ ions. *Opt. Mater.* **2012**, *34*, 2041–2044. [[CrossRef](#)]

17. Shunkeyev, K.; Myasnikova, L.; Barmina, A.; Zhanturina, N.; Sagimbaeva, S.C.; Aimaganbetova, Z.; Sergeyev, D. The thermostimulated luminescence of radiation defects in KCl, KBr and KI crystals at elastic and plastic deformation. *J. Phys. Conf. Ser.* **2017**, *830*, 012138. [[CrossRef](#)]
18. Zhanturina, N.; Sergeyev, D.; Aimaganbetova, Z.; Zhubaev, A.; Bizhanova, K. Features of the Spectroscopic Characteristics of Yttrium-Aluminum Garnets Doped with Europium at Different Concentrations. *Crystals* **2023**, *13*, 702. [[CrossRef](#)]
19. Boronat, C.; Rivera, T.; Garcia-Guinea, J.; Correcher, V. Cathodoluminescence emission of REE (Dy, Pr and Eu) doped LaAlO₃ phosphors. *Radiat. Phys. Chem.* **2017**, *130*, 236–242. [[CrossRef](#)]
20. Piramidowicz, R.; Jusza, A.; Lipińska, L.; Gil, M.; Mergo, P. Re³⁺:LaAlO₃ doped luminescent polymer composites. *Opt. Mater.* **2019**, *87*, 35–41. [[CrossRef](#)]
21. Troster, T.; Schweizer, S.; Secu, M.; Spaeth, J.-M. Luminescence of BaBr₂:Eu²⁺ under hydrostatic pressure. *J. Lumin.* **2002**, *99*, 343–347. [[CrossRef](#)]
22. Mahlik, S.; Lazarowska, A.; Grinberg, M.; Wells, J.-P.R.; Reid, M.F. Luminescence properties of MgF₂:Yb²⁺ at High Hydrostatic pressure. *J. Lumin.* **2015**, *169*, 788–793. [[CrossRef](#)]
23. Su, F.; Ma, B.; Ding, K.; Li, G.; Wang, S.; Chen, W.; Joly, A.G.; McCready, D.E. Luminescence temperature and pressure studies of Zn₂SiO₄ phosphors doped with Mn²⁺ and Eu³⁺ ions. *J. Lumin.* **2006**, *116*, 117–126. [[CrossRef](#)]
24. Winskiewski, K.; Mahlik, S.; Grinberg, M.; Seo, H.J. Influence of high hydrostatic pressure on Eu²⁺-luminescence in KMgF₃:Eu²⁺ crystal. *J. Lumin.* **2011**, *131*, 306–309. [[CrossRef](#)]
25. Mahlik, S.; Malinowski, M.; Grinberg, M. High pressure and time resolved luminescence spectra of Gd₃Ga₅O₁₂:Pr³⁺ crystal. *Opt. Mater.* **2011**, *3*, 1525–1529. [[CrossRef](#)]
26. Behrendt, M.; Mahlik, S.; Grinberg, M.; Stefańska, D.; Dereń, P.J. Influence of charge transfer state on Eu³⁺ luminescence in LaAlO₃ by high pressure spectroscopy. *Opt. Mater.* **2017**, *63*, 158–166. [[CrossRef](#)]
27. Baran, A.; Mahlik, S.; Grinberg, M.; Zych, E. High pressure and time-resolved luminescence spectra of Ca₃Y₂(SiO₄)₃ doped with Eu²⁺ and Eu³⁺. *J. Phys. Conf. Ser.* **2013**, *25*, 025603.

Disclaimer/Publisher's Note: The statements, opinions and data contained in all publications are solely those of the individual author(s) and contributor(s) and not of MDPI and/or the editor(s). MDPI and/or the editor(s) disclaim responsibility for any injury to people or property resulting from any ideas, methods, instructions or products referred to in the content.